3D STRUCTURES WITH PIEZORESISTIVE SENSORS IN STANDARD CMOS

E. Hoffman, B. Warneke, E. Kruglick, J. Weigold, K.S.J. Pister
UCLA Electrical Engineering, Los Angeles, CA 90024-1594 USA

Abstract

Aluminum hinges and polysilicon piezoresistors have been fabricated in a standard commercial CMOS process with one maskless post-processing step. The hinges and piezoresistors are formed using the metal interconnect and transistor gate layers in the CMOS process. Xenon difluoride is shown to be a simple and effective alternative to standard bulk etchants for this process, because of its extreme selectivity and gentle gas phase etch. Preliminary results from a piezoresistive accelerometer are given.

Introduction

Application development in MEMS is often hampered by process related barriers. Even 'proof-of-concept' designs can take a substantial amount of process development time. The development of a device (mask) design is typically tightly coupled to process parameters, so the process designer and the application designer need to be in close communication, if not be the same person.

This is sharply contrasted with the state of integrated circuit design, in which it is possible to design good circuits (although perhaps not the best circuits) with little or no knowledge of the fabrication process. In fact, with scalable CMOS design rules, digital circuits can be designed to be fabricated in an entire class of processes, with substantially different design rules and device parameters.

If a given MEMS process can be shown to have a wide set of applications, and a large palette of devices, it will open the way for engineers and scientists from other disciplines to create new MEMS systems and applications. Post processed foundry CMOS has the potential to become such a process.

Several groups in Europe and North America have demonstrated that it is possible to micromachine commercial CMOS using maskless post-processing. This is done by stacking an active area, both metal contact cuts, and the overglass cut to leave bare silicon exposed when the chips return from the foundry [10]. The chips are then etched in EDP, or some other anisotropic etchant. This technique was demonstrated in the late 1980s [12], and has since been used to produce a wide variety of MEMS components, including IR emitting arrays for thermal scene simulation [13], thermopile converters [4], thermal actuators [14], flow sensors [11], and resonant hygrometers [2] [1].

Additionally, foundry CMOS has been used to make high voltage devices [15], absolute temperature sensors [9], and visible light imaging arrays. This impressive list of sensors and actuators comes packaged along with all of the analog and digital electronics available in the process. Two limitations of this approach have been the constraints imposed by etching and limited structural components.

Fabrication

The devices shown here were fabricated through the MOSIS foundry service using Orbit Semiconductor's 2 micron double poly double metal CMOS processes. Devices were fabricated in both N-well and P-well technologies.

All lithography and thin film patterning is performed during the normal course of the CMOS process. When the chips return from the foundry, they require a single unmasked etch. The traditional EDP etch is useful for etching pits and structures with dimensions on the order of 100 microns, but for longer etches the aluminum metalization in the bonding pads is destroyed. Hydrazine monohydrate has been proposed as a higher selectivity etchant [5], but the hazards of this material are substantially worse than EDP, which itself must be treated with caution.

We have experimented with two etchants, xenon difluoride, and tetramethyl ammonium hydroxide.

Xenon Difluoride

Xenon difluoride (XeF_2), is a white solid which sublimates at room temperature with a vapor pressure of roughly 4 Torr. XeF_2, first synthesized in the early 1960s [6], is commercially available through several sources [8].

The etching apparatus is quite simple (Fig. 3), consisting of a chamber, vacuum pump, and source bottle. The etch is performed in vapor phase, at room temperature, with no external energy sources, at between 1 and 4 Torr. Under these conditions, we have observed silicon etch rates as high as ten microns per minute, although 1-3 microns per minute is more typical. Samples with less exposed silicon etch faster. The etch is nearly isotropic, and leaves a surface roughness of several microns (Fig. 2). There is

0-7803-2503-6 © 1995 IEEE

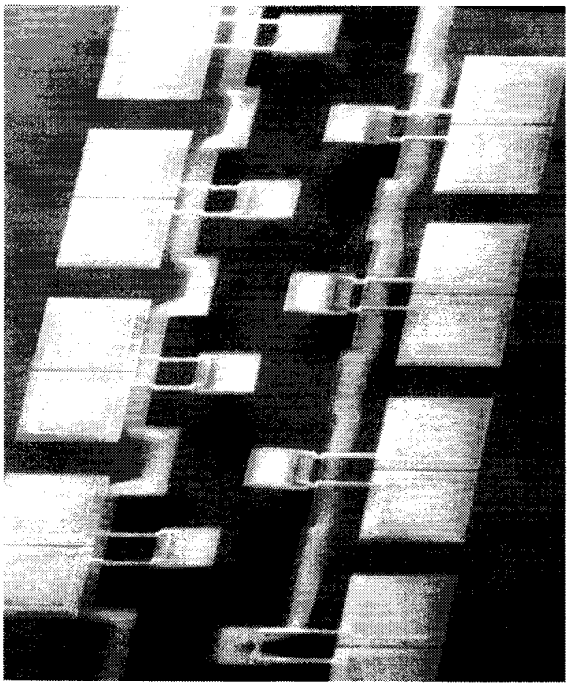

Figure 1: Structures etched in XeF2. The plates are composed of a 4 layer stack of oxides, 3 μm thick and 80 μm square. They are suspended on 5 μm wide, 1.1 μm thick aluminum beams.

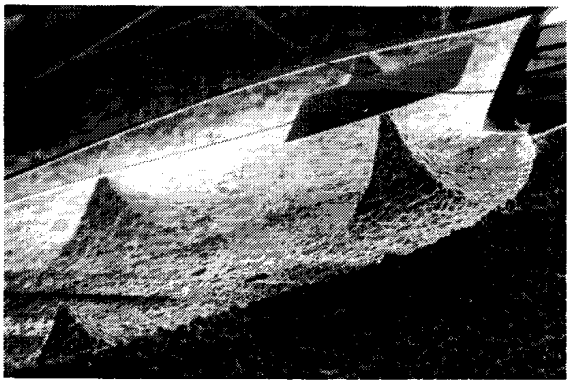

Figure 2: Side view of a typical etch pit after XeF_2 etch. The suspended oxide plate is 200 μm square.

an aperture effect: areas etched through small holes etch somewhat slower than large areas of exposed silicon.

The extreme selectivity of XeF_2 to silicon dioxide and silicon nitride are documented [7, 19]. A 40 nm gate oxide is sufficient to protect a polysilicon gate from underside etch. We have shown that XeF_2 is also extremely selective to aluminum, and photoresist. Single-mask test structures made from 50 nm thick aluminum have been successfully released. A single layer of hardbaked photoresist makes an excellent etch mask. Chips bonded in standard ceramic chip carriers have been etched and tested successfully.

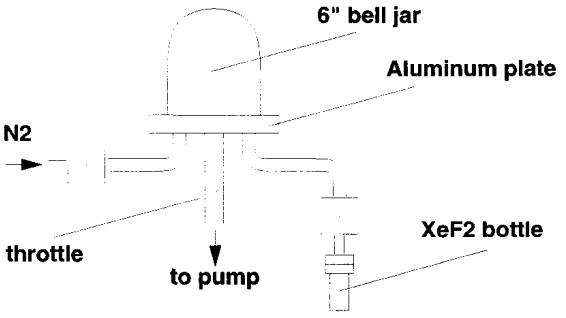

Figure 3: The XeF2 etching system consists of a machined aluminum plate with several attachment sites for pump, N2 purge, XeF2 source, and capacitance manometer (not shown). Etching is typically performed with the N2 line shut, the XeF2 valve open, and the pump throttled to provide an etching pressure of 1 Torr.

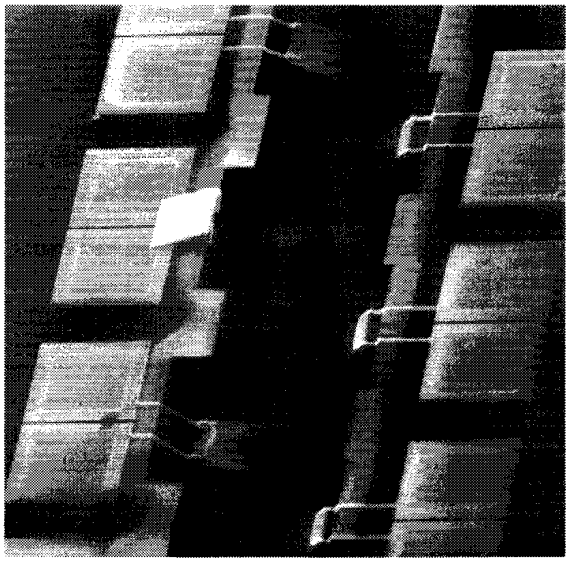

Figure 4: Structures etched in TMAH/silicic acid. These structures are identical to those shown in Fig. 1. Aluminum beams have deformed plastically during the etch and drying process.

The vapor phase etch is quite gentle, and delicate structures survive with no special precautions. The CMOS electronics is not affected by this etchant, and

several op-amps and other analog circuits have been etched and successfully operated.

TMAH and Silicic Acid

Silicon doping of tetramethyl ammonium hydroxide (TMAH) solutions has been demonstrated as a method for improving selectivity of TMAH to aluminum [17]. By adding silicic acid directly, we have seen similar results. The samples shown in Fig. 4 were etched in a solution of 80 ml of 25% TMAH, 16 gm of silicic acid, and balance DI water in a 250 ml beaker. The chip was etched at 70C for 24 hours, with a resulting etch depth of between 50 and 100 microns, varying with surface pattern. As can be seen from Fig. 4, the etch is nearly isotropic. The main difference between the structures etched in the (liquid) TMAH/silicic acid and the structures etched in the (gas) XeF2 is the drying-induced bending of all of the support beams.

Results

The devices described below are based on two key elements illustrated in Fig. 5, the aluminum beam and the polysilicon strain gauge. The aluminum beam acts as a plastically deformable flexural hinge, similar to the polyimide hinges demonstrated by Suzuki, et al. [18]. The hinge is created by running a line of metal over bare silicon, and the strain gauge consists of a polysilicon resistor protected from the etch by the surrounding oxides. A typical CMOS process will have an additional layer of metal and polysilicon not shown in Fig. 5. In a two metal process, only the second metal is appropriate for hinges, as the first layer will be substantially removed by the overetch of the second. Similarly, much of the silicon substrate in the 'open' areas is removed by the overetch of the oxide and metal layers, resulting in metal traces which are recessed into the substrate after fabrication.

Once the structure has been etched, the oxide plates and aluminum beams will be suspended over silicon pits. The multi-layer structures are generally surprisingly flat, considering the heterogeneity of the thin films. Strain gradient induced deflections are typically less than ten microns for cantilevers with lengths less than three hundred microns. On a recent run, however, the tip deflection of a 300 micron oxide cantilever was over 100 microns. This excessive curvature is generally undesirable.

The resistance of the loops of aluminum shown in Figs. 1 and 4 is constant at between one and two

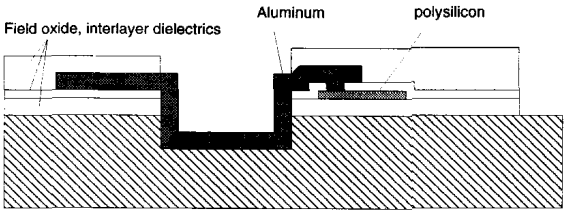

Figure 5: Simplified cross section of an aluminum trace running between oxide plates and contacting a polysilicon piezoresistor. The oxide and first metal overetch into the silicon substrate causes the aluminum to be lower than the oxides.

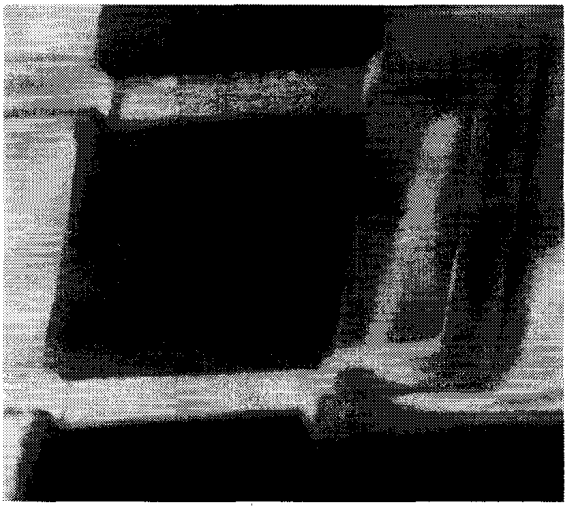

Figure 6: An aluminum trace (second metal) running between oxide plates. The conductivity of the metal is unaffected by the XeF2 etch.

ohms before and after the etch. The aluminum can be deformed elastically over a small range of motion, and then deforms plastically. Beams are rotated using mechanical probes, and can be rotated well past 90 degrees. The resistance of the plastically deformed aluminum lines also remains constant at between one and two ohms, even after several deformations. Aluminum lines fail at current densities above 10 $mA/\mu m^2$, before and after etch.

Polysilicon strain gauges were characterized using several different beam and plate geometries. The n-type gauge factor was found to vary between -10 and -20 over several runs tested.

Figure 7 shows the design of two variations of an accelerometer test structure. The basic design is a proof mass composed of an oxide plate, typically with etch holes, and one or more support beams which

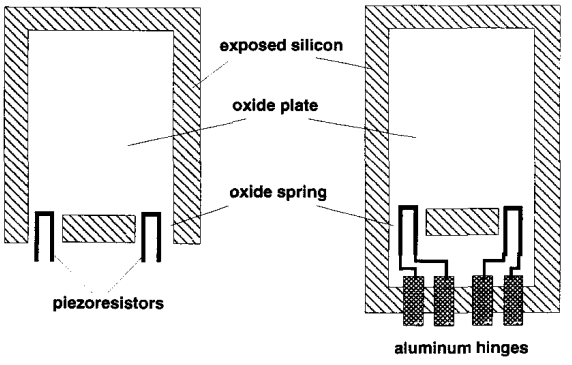

Figure 7: Two accelerometer designs. The left design detects acceleration normal to the plane of the wafer. The right design can be rotated out of the plane of the wafer, to detect orthogonal accelerations.

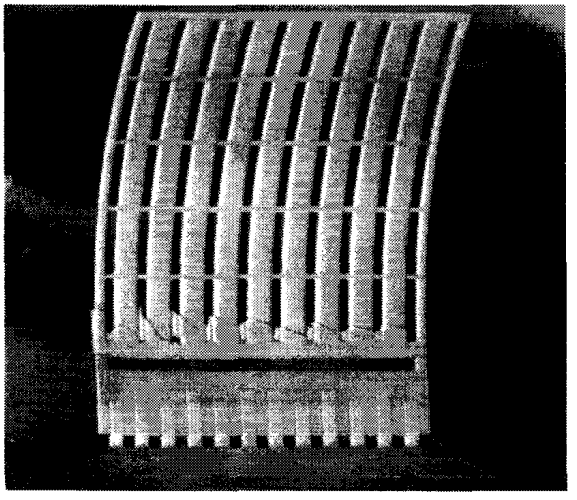

Figure 8: SEM of a piezoresistive accelerometer, rotated out of the plane of the wafer on aluminum hinges. The hinges provide both mechanical support and electrical connectivity between the strain gauges and the wafer surface. Overall dimensions are 500x650μm^2. The aluminum hinges are 20 μm wide.

contain polysilicon piezoresistors. Metal and poly layers can be used to increase the mass. By adding a support plate and aluminum hinges, this design can be rotated out of the plane of the wafer, as shown in Fig. 8. The resistance change was measured as a function of tip displacement for these devices. A probe was used to deflect the tip of the plate, and the deflection was measured visually, using the microscope focus for the vertical displacement. The results are shown in Figs. 9 and 10. Note that the electrical connection to the resistor measured in Fig 10 is made through two aluminum hinges.

The resistance of the accelerometer strain gauges was measured using a $5\frac{1}{2}$ digit DVM, and the reading at any deflection was stable out to the last digit, which tended to drift over periods of tens of seconds. A wire-wrapped amplifier board was built with a gain of 1000 and a bandwidth from DC to 10 Hz. The total RMS input noise of the amplifier was roughly 5-10 μV. Using a Wheatstone bridge configuration with a half bridge on-chip, the external amplifier showed a 20 mV change when the accelerometer was rolled over from +1g to -1g. Given the geometry of the accelerometer and layer thickness estimates, this output signal is within the expected range. The 10 mV/g output signal corresponds to deflection in the tens of nm/g.

A three axis version of the accelerometer was designed using one planar accelerometer and two orthogonal hinged accelerometers, each with an integrated low noise CMOS amplifier. Each proof mass is composed of a stack of all oxides and conductors (total mass 2.5 μgm). The support beams contain a 1kΩ polysilicon piezoresistor. The total area of the three axis system was four square millimeters. The devices were fabricated, but could not be tested because of a design flaw in the bonding pad ring. Based on measured performance of the sensors and simulated performance of the amplifiers, these accelerometers with integrated CMOS amplifiers should provide substantially better performance than the off-chip amplified accelerometer.

Rotated structures can be made with interlocking braces to keep the structures in the desired position, similar to the techniques used with polysilicon structures [16]. With no external loading, the structures shown in Fig. 11 stand on their own, held in place by aluminum hinges. A micromanipulator or other external force can be used to bend the hinges back down, however. A tab in slot brace was designed to fit on either side of the assembled structure. With the brace in place, a micromanipulator was used to try to force the structure back down, and the oxide beam snapped before the brace failed. The oxide snapped at the base of the neck, close to the base plate.

Fig. 12 shows a structure designed to have a rigid structural cage supporting a flexible deflection plate for gap closing experiments. The outer cage beams are built with polysilicon, metal, and oxide layers and are intended to be rigid. The central deflection plate was pushed down part way to the surface

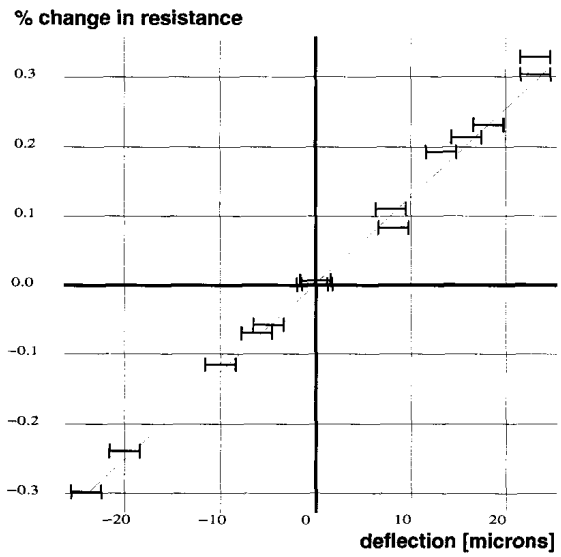

Figure 9: Resistance change vs. vertical deflection for a surface accelerometer.

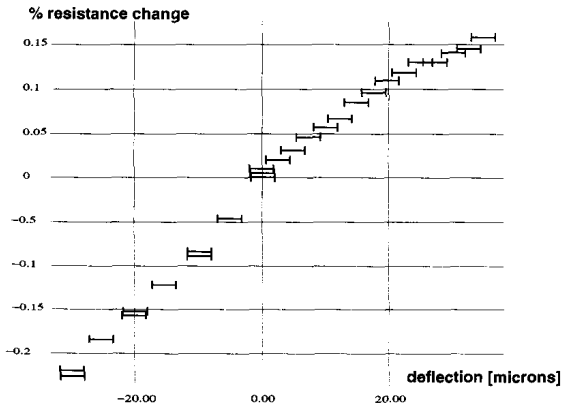

Figure 10: Resistance change vs. horizontal deflection for the accelerometer shown in Figure 8.

with a micromanipulator, after which the plate could be deflected repeatedly with an applied potential of twelve volts. During actuation of the central plate the outer rigid support cage showed no evidence of deformation.

Conclusion

A wide variety of sensors and actuators has previously been demonstrated using simple post-processing of standard CMOS. It is now also possible to assemble simple three dimensional structures with integral piezoresistive deflection and force sensors.

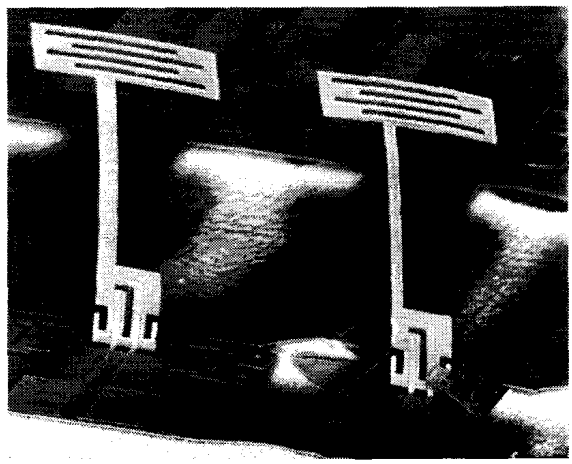

Figure 11: 2 deflection test structures. Note the two braces at the base of the right anemometer. The anemometers are 300 microns tall.

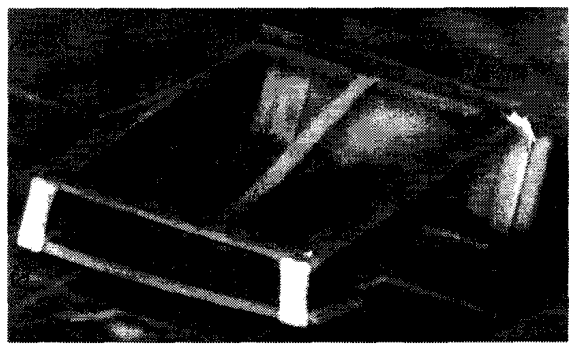

Figure 12: A box with central deflection plate. The box is 100 microns square and designed to be 40 microns tall. The central spring-supported plate was pushed down by a probe.

Additionally, a simple new gas phase approach to CMOS post-process etching has been demonstrated. With this extensive set of micro electromechanical elements, coupled with the overwhelming electrical capabilities available in CMOS, it should soon be possible to design and fabricate sophisticated systems and applications with very rapid turnaround time.

Layout for the structures pictured in this paper is available by anonymous ftp and http from synergy.icsl.ucla.edu (128.97.90.45).

Acknowledgments

Many thanks to Eli Yablonovitch for seminal discussions on selective silicon etching; to Mike Hecht of JPL for advice and help building the first XeF_2

test setup; to Gisela Lin for etching and SEM work; and to Beverley Eyre for breaking a cantilever and exposing the first aluminum hinge.

References

[1] Henry Baltes. CMOS as sensor technology. *Sensors and Actuators (A)*, 37-38:51–56, 1993.

[2] T. Boltshauser, A. Haberli, and H. Baltes. Piezoresistive membrane hygrometers based on IC technology. *Sensors and Materials*, 5(3):125–134, 1993.

[3] J.Y.C. Chang, A.A. Abidi, and M. Gaitan. Large suspended inductors on silicon and their use in a $2\mu m$ CMOS RF amplifier. *Electron Device Letters*, 14(5), May 1993.

[4] M. Gaitan, J. Kinard, and D. X. Huang. Performance of commerical CMOS foundry-compatible multijunction thermal converters. In *Proc. 7th Int. Conf. on Solid State Sensors and Actuators (Transducers '93)*, pages 1012–1014, Yokohama, June 7-10, 1993.

[5] M.A. Gajda, H. Ahmed, J.E.A. Shaw, and A. Putnis. Anisotropic etching of silicon in hydrazine. *Sensors and Actuators (A)*, 40:227–236, 1994.

[6] Herbert H. Hyman, editor. *Noble-Gas Compounds.* University of Chicago Press, 1963.

[7] D.E Ibbotson et al. Comparison of XeF2 and F-atom reactions with Si and SiO2. *Appl. Phys. Lett.*, 44(12):1129–1131, 1984.

[8] PCR Inc. P.O. Box 1466, Gainsville, FL 32602 USA.

[9] P. Krummenacher and H. Oguey. Smart temperature sensor in CMOS technology. *Sensors and Actuators*, A21-A23:636–638, 1990.

[10] J. Marshal et al. Realizing suspended structures on chips fabricated by CMOS foundry processes through the MOSIS service. NISTIR 5402, U.S. National Institute of Standards and Technology, Gaithersburg, MD 20899, June 1994.

[11] David Moser. *CMOS flow sensors.* PhD thesis, ETH Zurich, Physical Electronics Laboratory, Swiss Federal Institute of Technology, Zurich, 1993.

[12] M. Parameswaran, H.P. Baltes, Lj. Ristic, A.C. Dhaded, and A.M. Robinson. A new approach for the fabrication of micromachined structures. *Sensors and Actuators*, 19:289–307, 1989.

[13] M. Parameswaran, R. Chung, M. Gaitan, R.B. Johnson, et al. Commercial CMOS fabricated integrated dynamic thermal scene simulator. In *IEEE Int. Elec. Dev. Mtg., San Francisco, CA, Dec. 13-16*, pages 753–756, 1991.

[14] M. Parameswaran, Lj. Ristic, K. Chau, A.M. Robinson, and W. Allegretto. CMOS electrothermal microactuators. In *Proc. IEEE Micro Electro Mechanical Systems Workshop*, pages 128–131, Napa, CA, Feb. 11-14, 1990.

[15] Z. Parpia, , C. Andre, T. Salama, and R. Hadaway. Modelling of CMOS compatible high voltage device structures. In *Proc. Symp. High Voltage and Smart Power Devices*, pages 41–50, 1987.

[16] K.S.J. Pister. Hinged polysilicon structures with integrated thin film transistors. In *Proc. IEEE Solid State Sensor and Actuator Workshop*, pages 136–139, Hilton Head, South Carolina, June 22-25, 1992.

[17] U. Schnakenberg, W. Benecke, and P. Lange. TMAHW etchants for silicon micromachining. In *Proc. 6th Int. Conf. on Solid State Sensors and Actuators (Transducers '91)*, pages 815–818, San Francisco, June 1991.

[18] K. Suzuki, I. Shimoyama, H Miura, and Y. Ezura. Creation of an insect-based microrobot with an external skeleton and elastic joints. In *Proc. IEEE Micro Electro Mechanical Systems Workshop*, pages 190–195, Travemunde, Germany, February 4-7, 1992.

[19] H.F. Winters and J.W. Coburn. The etching of silicon with XeF2 vapor. *Appl. Phys. Lett.*, 34(1):70–73, 1979.